Impact of anthropogenic atmospheric nitrogen and sulfur deposition on ocean acidification and the inorganic carbon system

Scott C. Doney*†, Natalie Mahowald‡, Ivan Lima*, Richard A. Feely§, Fred T. Mackenzie¶, Jean-Francois Lamarque‖, and Phil J. Rasch‡

*Marine Chemistry and Geochemistry Department, Woods Hole Oceanographic Institution, 266 Woods Hole Road, Woods Hole, MA 02543; Divisions of ‡Climate and Global Dynamics and ‖Atmospheric Chemistry, National Center for Atmospheric Research, 1850 Table Mesa Drive, Boulder, CO 80303; §Pacific Marine Environmental Laboratory, National Oceanic and Atmospheric Administration, 7600 Sand Point Way NE, Seattle, WA 98115-6349; and ¶Department of Oceanography, School of Ocean and Earth Science and Technology, University of Hawaii at Manoa, 100 Pope Road, Honolulu, HI 96822

Edited by Michael L. Bender, Princeton University, Princeton, NJ, and approved July 9, 2007 (received for review March 9, 2007)

Fossil fuel combustion and agriculture result in atmospheric deposition of 0.8 Tmol/yr reactive sulfur and 2.7 Tmol/yr nitrogen to the coastal and open ocean near major source regions in North America, Europe, and South and East Asia. Atmospheric inputs of dissociation products of strong acids (HNO_3 and $H2SO_4$) and bases (NH_3) alter surface seawater alkalinity, pH, and inorganic carbon storage. We quantify the biogeochemical impacts by using atmosphere and ocean models. The direct acid/base flux to the ocean is predominately acidic (reducing total alkalinity) in the temperate Northern Hemisphere and alkaline in the tropics because of ammonia inputs. However, because most of the excess ammonia is nitrified to nitrate (NO_3^-) in the upper ocean, the effective net atmospheric input is acidic almost everywhere. The decrease in surface alkalinity drives a net air–sea efflux of CO_2, reducing surface dissolved inorganic carbon (DIC); the alkalinity and DIC changes mostly offset each other, and the decline in surface pH is small. Additional impacts arise from nitrogen fertilization, leading to elevated primary production and biological DIC drawdown that reverses in some places the sign of the surface pH and air–sea CO_2 flux perturbations. On a global scale, the alterations in surface water chemistry from anthropogenic nitrogen and sulfur deposition are a few percent of the acidification and DIC increases due to the oceanic uptake of anthropogenic CO_2. However, the impacts are more substantial in coastal waters, where the ecosystem responses to ocean acidification could have the most severe implications for mankind.

alkalinity | biogeochemistry | global change | ocean chemistry | nutrient eutrophication

Humans are dramatically altering the global nitrogen and sulfur budgets, with one result being the release of large fluxes of nitrogen oxides (NO_x, ≈2 Tmol/yr), ammonia (NH_3, ≈4 Tmol/yr), and sulfur dioxide (SO_2, ≈2 Tmol/yr) to the atmosphere (1). Globally, fossil fuel combustion and biomass burning fluxes of NO_x exceed the natural fluxes from land to the atmosphere (2); NH_3 fluxes to the atmosphere are overwhelmed by those from human activities, mainly livestock husbandry (3); and oxidized sulfur fluxes from land are ≈10 times the natural fluxes, again because of combustion of fossil fuels and biomass burning (2). After chemical transformations in the atmosphere, much of the anthropogenic nitrogen and sulfur is deposited to the surface as the dissociation products of nitric acid (HNO_3) and sulfuric acid (H_2SO_4). HNO_3 and H_2SO_4 are strong acids that completely dissociate in water:

$$HNO_3 \rightarrow H^+ + NO_3^- \quad \text{and} \quad H_2SO_4 \rightarrow 2H^+ + SO_4^{2-}. \qquad [1]$$

Because of the relatively short lifetime of reactive nitrogen and sulfur species in the atmosphere (days to about a week), the majority of the acid deposition occurs on land, in the coastal ocean, and in the open ocean downwind of the primary source regions in eastern North America, Europe, and South and East Asia (4–7). The subsequent acidification of terrestrial and freshwater ecosystems by dry deposition and more acidic rainfall is a well known environmental problem (8–11).

Anthropogenic nitrogen and sulfur deposition to the ocean surface alters surface seawater chemistry, leading to acidification and reduced total alkalinity. Lower pH and resulting lower CO_3^{2-} concentrations are of particular concern for a range of benthic and pelagic organisms that form calcareous ($CaCO_3$) shells (e.g., corals, coralline algae, foraminifera, pteropods, and coccolithophores) (12, 13). The acidification effects, although not as large globally as those of anthropogenic CO_2 uptake (14, 15), could be significant in coastal ocean regions because these regions are already vulnerable to other human impacts, including nutrient fertilization (15, 16), pollution, overfishing, and climate change. Here we compute bounds on the potential impact of anthropogenic nitrogen and sulfur deposition on seawater chemistry, using simulated atmospheric deposition fields applied to a coupled 3D ocean ecosystem–biogeochemical model (see *Methods*). We also compare these model results with field observations for U.S. coastal regions.

Basic Principles of the Effects of Atmospheric C, N, and S Deposition on Seawater Chemistry. It is useful to frame the impact of anthropogenic nitrogen and sulfur inputs in terms of the changes in surface water dissolved inorganic carbon (DIC) and total alkalinity (Alk). DIC and Alk are conservative quantities with respect to mixing and temperature and pressure changes and, together with temperature and salinity, determine seawater pH and the partial pressure of carbon dioxide, pCO_2 (17), an important factor driving air–sea CO_2 exchange. Processes that increase DIC or decrease Alk lower seawater pH (ocean acidification) and raise pCO_2.

CO_2 combines with water to form carbonic acid (H_2CO_3), which then undergoes a series of acid/base dissociation reactions:

$$CO_2(aq) + H_2O \leftrightarrow H_2CO_3 \leftrightarrow H^+ + HCO_3^- \leftrightarrow 2H^+ + CO_3^{2-}. \qquad [2]$$

DIC concentration ([DIC]; μmol/kg) is

Author contributions: S.C.D. and N.M. designed research; S.C.D., N.M., and I.L. performed research; J.-F.L. and P.J.R. contributed new reagents/analytic tools; S.C.D., N.M., and I.L. analyzed data; and S.C.D., N.M., R.A.F., and F.T.M. wrote the paper.

The authors declare no conflict of interest.

This article is a PNAS Direct Submission.

Freely available online through the PNAS open access option.

Abbreviations: Alk, total alkalinity; DIC, dissolved inorganic carbon.

†To whom correspondence should be addressed. E-mail: sdoney@whoi.edu.

$$[\mathrm{DIC}] = [\mathrm{CO_2(aq)}] + [\mathrm{H_2CO_3}] + [\mathrm{HCO_3^-}] + [\mathrm{CO_3^{2-}}]. \quad [3]$$

Anthropogenic CO_2 uptake increases surface [DIC] and lowers pH (14, 18).

Total alkalinity ([Alk]; μeq/kg), a measure of the acid/base balance of the fluid (19), is defined conventionally as the excess of proton acceptors (bases formed from weak acids) over proton donors relative to a reference point (formally, acid dissociation $pK_a = 4.5$; approximately the H_2CO_3 equivalence point):

$$[\mathrm{Alk}] = -[\mathrm{H^+}] + [\mathrm{OH^-}] + [\mathrm{HCO_3^-}] + 2[\mathrm{CO_3^{2-}}] + [\mathrm{NH_3}] + \text{minor species}, \quad [4]$$

or, alternatively, as the net positive charge from strong mineral bases minus strong mineral acids (20):

$$[\mathrm{Alk}] = [\mathrm{Na^+}] + [\mathrm{K^+}] + 2[\mathrm{Ca^{2+}}] + 2[\mathrm{Mg^{2+}}] - [\mathrm{Cl^-}] - 2[\mathrm{SO_4^{2-}}] - [\mathrm{NO_3^-}]. \quad [5]$$

In Eq. **4**, we neglect for clarity terms from other weak acids in seawater, such as $B(OH)_3$, H_2SiO_3, and $H_2PO_4^-$, which are included in our seawater thermodynamics code (21).

Atmospheric C, N, and S inputs can be converted into fluxes of inorganic carbon, fDIC (mol·m^{-2}·y^{-1}), and alkalinity, fAlk (eq·m^{-2}·y^{-1}). The fDIC flux

$$f\mathrm{DIC} = f\mathrm{CO_2^{gas}} + f\mathrm{C_{organic}} + f\mathrm{CaCO_3} + f\mathrm{DIC^{rain}} \quad [6]$$

is governed by CO_2 air–sea gas exchange $f\mathrm{CO_2^{gas}}$, net respiration of atmospheric dissolved and particulate organic matter inputs $f\mathrm{C_{organic}}$, and net dissolution of $CaCO_3$ from atmospheric dust deposition $f\mathrm{CaCO_3}$, as well as by dissolution of DIC in rainwater $f\mathrm{DIC^{rain}}$, a small term that is usually neglected. The anthropogenic changes in $f\mathrm{C_{organic}}$ and $f\mathrm{CaCO_3}$ are not well characterized and are not considered further here.

The chemical forms of the atmospheric C, N, and S inputs are important for determining their impact on the alkalinity flux:

$$f\mathrm{Alk} = 2f\mathrm{Ca^{2+}} - 2f\mathrm{SO_2} - 2f\mathrm{SO_4^{2-}} - f\mathrm{NO_3^-} + f\mathrm{NH_3} + f\mathrm{NH_4^+}. \quad [7]$$

Dissolution of calcareous mineral dust, $CaCO_3$, in rainwater, denoted by the input of dissolved Ca^{2+} ion in Eq. **7**, acts to add alkalinity to the surface ocean (fAlk > 0). Note the factor of 2 conversion for alkalinity, reflecting the charge on Ca^{2+} and CO_3^{2-} (Eqs. **4** and **5**). Air–sea CO_2 gas exchange, the pathway for almost all anthropogenic carbon input to the ocean, does not enter Eq. **7** because adding CO_2 does not alter ocean total alkalinity (Eq. **4**) but does change carbonate alkalinity ($\mathrm{Alk_{carb}} = [\mathrm{HCO_3^-}] + 2[\mathrm{CO_3^{2-}}]$) (22). Similarly, the release of CO_2 from organic carbon respiration does not affect alkalinity except through related conversion of organic nitrogen (and to an even smaller extent phosphorus) to inorganic form.

Inorganic sulfur deposition adds acidity to the surface ocean (fAlk < 0), reducing surface water alkalinity. About 40–80% of atmospheric S is oxidized to H_2SO_4 by gas-phase and aqueous reactions and deposited to the surface by wet (dominant) and dry processes. An input of 1 mole SO_4^{2-} is equivalent to -2 equivalents Alk. The remaining sulfur emissions are dry-deposited as SO_2. We assume for surface seawater that all of the SO_2 combines with water to form H_2SO_4 and thus has a similar effect on alkalinity as SO_4^{2-} deposition.

Atmospheric nitrogen deposition can add either acidity or alkalinity, depending on the chemical form. The wet deposition of NO_3^- is acidic, and the dry deposition of NH_3 is alkaline (Eqs. **4** and **5**). From Eq. **4**, one might expect that wet deposition of the ammonium ion NH_4^+ should result in no change in alkalinity because the protonated species is the primary form at the CO_2 equivalence pH (pK_a of NH_4^+ for seawater $\approx$9.5). However, in rainwater the main proton source for forming the ammonium ion is water, and the resulting release of OH^- increases alkalinity similar to NH_3 deposition. A fraction of the atmospheric N and S is deposited as ammonia–sulfate aerosols, $(NH_4)_2SO_4$ and $(NH_4)HSO_4$; in our calculations we assume that the aerosols dissociate in surface seawater and include the aerosol N and S in the NH_4^+ and SO_4^{2-} fluxes. Our alkalinity flux (Eq. **7**) is similar to the atmosphere acidity equation for wet deposition from ref. 6, although of course with opposite signs. One difference is that we include additional SO_2 and NH_3 terms because of dry deposition.

The impact of atmospheric $NH_4^+ + NH_3$ input on ocean alkalinity depends on the extent to which the NH_4^+ is converted to NO_3^- by nitrification:

$$\mathrm{NH_4^+} + 2\mathrm{O_2} \rightarrow \mathrm{NO_3^-} + 2\mathrm{H^+} + \mathrm{H_2O}. \quad [8]$$

Note that almost all of the deposited NH_3 will be converted to NH_4^+ at seawater pH. Nitrification reduces alkalinity by 2 equivalents for every mole of NH_4^+ consumed. Assuming complete nitrification changes the alkaline NH_3 and NH_4^+ flux to an effective acidity flux:

$$f\mathrm{Alk_{nitrif}} = 2f\mathrm{Ca^{2+}} - 2f\mathrm{SO_2} - 2f\mathrm{SO_4^{2-}} - f\mathrm{NO_3^-} - f\mathrm{NH_3} - f\mathrm{NH_4^+}. \quad [9]$$

As shown below in our 3D ocean simulations, Eq. **9** is a good approximation when examining ocean alkalinity inventory changes because $\approx$98% of anthropogenic $NH_3 + NH_4^+$ deposition is nitrified to NO_3^-. When referring to atmospheric precipitation, the inclusion of nitrification is often termed potential acidity (19). For the spatial flux maps below (Fig. 1), we compute both fAlk and $f\mathrm{Alk_{nitrif}}$.

Results and Discussion

Model atmospheric nitrogen, sulfur, and alkalinity deposition fields are computed based on estimated changes in climate and emissions between the preindustrial and current climates (1990–2000) (Fig. 1) (see *Methods*). The global Community Climate System Model 3 (CCSM-3) nitrogen and sulfur deposition fluxes (Table 1) are similar to the results reported in the 2001 Intergovernmental Panel on Climate Change report (1, 23). For comparison, air–sea CO_2 fluxes are reported from the CCSM-3 ocean model.

About one-third of anthropogenic NO_x and SO_x emissions, mostly from fossil fuel combustion, are deposited to the ocean. Because of the short atmospheric residence time, deposition is concentrated downwind of the emission sources, mostly in the temperate North Atlantic, temperate and eastern subtropical North Pacific, and northern Indian Ocean, with maximum values approaching -0.03 mol·m^{-2}·y^{-1}. Approximately half of agricultural NH_x emissions are deposited to the ocean and are more evenly spread over the Northern Hemisphere.

The anthropogenic alkalinity flux fAlk is negative (acidic) in the temperate regions of the Northern Hemisphere dominated by fossil fuel $f\mathrm{SO_4^{2-}} + f\mathrm{SO_2}$ and $f\mathrm{NO_3^-}$ deposition and is positive (alkaline) in the tropics owing to $f\mathrm{NH_4^+} + f\mathrm{NH_3}$ deposition (Fig. 1 displays acidity, the negative of fAlk and $f\mathrm{Alk_{nitrif}}$, for comparison with other fluxes). On a global basis, the alkalinity reduction from $f\mathrm{SO_4^{2-}} + f\mathrm{SO_2}$ and $f\mathrm{NO_3^-}$ is largely canceled by $f\mathrm{NH_4^+} + f\mathrm{NH_3}$ inputs, and the global ocean integrated anthropogenic fAlk input is only -0.24 Teq·y^{-1}. Maximum deposition fluxes to the coastal ocean are -0.01 eq·m^{-2}·y^{-1}. Assuming complete nitrification of $f\mathrm{NH_4^+} + f\mathrm{NH_3}$ changes global ocean anthropogenic $f\mathrm{Alk_{nitrif}}$ input dramatically to -4.22 Teq·y^{-1}, with maximum coastal fluxes of -0.01 to -0.10 eq·m^{-2}·y^{-1}.

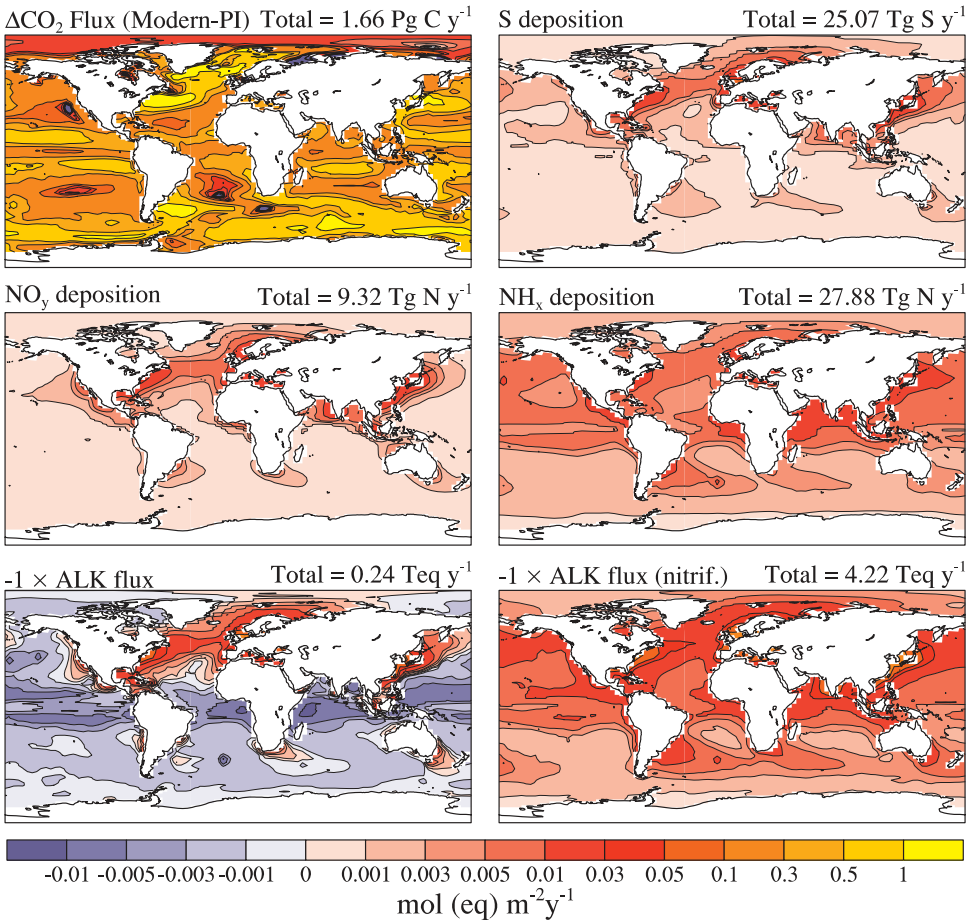

Fig. 1. Model-estimated anthropogenic (1990–2000 minus preindustrial) atmospheric deposition fluxes for carbon, nitrogen, and sulfur (mol·m^{-2}·y^{-1}); alkalinity; and potential alkalinity, assuming complete nitrification of $NH_4^+ + NH_3$ (eq·m^{-2}·y^{-1}).

Model ocean anthropogenic CO_2 uptake is 138 Tmol·y^{-1}, with spatial *f*DIC fluxes ranging from 0.1 to 2.0 mol C m^{-2}·y^{-1}. Highest anthropogenic *f*DIC values occur in regions of upwelling and water mass transformation (2, 24, 25). Globally, the ocean alkalinity reduction due to anthropogenic sulfur and nitrogen deposition, $f\text{Alk}_{\text{nitrif}}$, is at most, assuming full nitrification of ammonium deposition, approximately −3% of the *f*DIC inputs because of anthropogenic CO_2 uptake. However, the alkalinity fluxes can be significant relative to anthropogenic *f*DIC fluxes in some coastal ocean and margin areas. Previous modeling studies (Terrestrial Ocean Atmosphere Ecosystem Model, TOTEM; refs. 26 and 27) estimate anthropogenic atmospheric nitrogen deposition to the global coastal ocean of 0.03 mol·m^{-2}·y^{-1} for the turn of the 21st century, very similar to the estimates in Table 1. It was also shown that this flux will increase significantly during the next several decades, as will the reactive nitrogen flux to the coastal ocean from anthropogenic sources via rivers and groundwaters.

The anthropogenic alkalinity perturbation is redistributed by ocean circulation and initiates feedbacks by means of alterations in surface pH, air–sea CO_2 flux, and [DIC]. Biogeochemical transformations must also be considered because of nitrogen buildup or eutrophication of surface waters, stimulating increased ocean primary production and organic matter export (27–30). We evaluate the responses by using a 3D marine physical/ecological/biogeochemical model (see *Methods*), focusing on three sensitivity

Table 1. Model-estimated anthropogenic (1990–2000 minus preindustrial) and preindustrial atmospheric deposition fluxes

	Integrated anthropogenic deposition, Tmol/y or Teq/y (preindustrial)		Anthropogenic coastal ocean flux, mol or eq·m^{-2}·y^{-1}	
Flux	Global	Ocean-only	Model	Observed
fCO_2	—	138	0.10 to 2.00	
$fNH_4^+ + fNH_3$	4.11 (0.00)	1.99 (0.00)	0.00 to 0.03	0.02
fNO_3^-	1.84 (1.18)	0.67 (0.73)	0.00 to 0.03	0.02
$fSO_4^{2-} + fSO_2$	2.21 (0.58)	0.78 (0.49)	0.00 to 0.03	0.01
*f*Alk	−2.15 (−2.34)	−0.24 (−1.71)	−0.01 to +0.01	
$f\text{Alk}_{\text{nitrif}}$	−10.37 (−2.34)	−4.22 (−1.71)	−0.01 to −0.10	

Field observations are shown for comparison (4, 5).

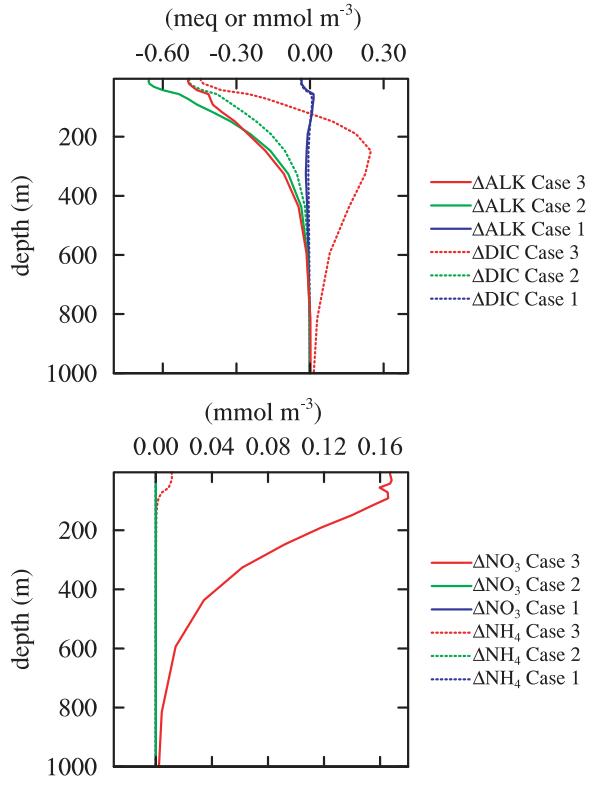

Fig. 2. Perturbations to simulated global vertical profiles due to 10 years of anthropogenic atmospheric nitrogen and sulfur deposition. (*Upper*) Alkalinity (solid lines) and DIC (dashed lines). (*Lower*) NO_3^- (solid lines) and NH_4^+ (dashed lines). Case 1 is forced with alkalinity flux from Fig. 1, case 2 with the potential alkalinity flux (assuming complete nitrification), and case 3 with alkalinity and nitrogen fluxes allowing for biological feedbacks.

experiments. Case 1 simulates direct alkalinity perturbations with no nutrient fertilization; fAlk alters surface [Alk]. Case 2 is similar to case 1, except assuming complete nitrification of $fNH_4^+ + fNH_3$; $f\text{Alk}_{\text{nitrif}}$ alters surface [Alk]. Case 3 incorporates explicit nitrogen cycle perturbations and allows for nutrient fertilization; fAlk alters surface [Alk], fNO_3^- alters surface $[NO_3^-]$, and $fNH_4^+ + fNH_3$ alters surface $[NH_4^+]$. All cases and a control (no atmospheric nitrogen and sulfur deposition) are integrated from 1990 to 2000, with repeat annual physics and increasing anthropogenic atmospheric CO_2 based on observations.

The direct effects of anthropogenic nitrogen and sulfur deposition in case 1 are small, in global integral, because alkalinity reductions from fNO_3^- and $fSO_4^- + fSO_2$ are nearly balanced by increases from $fNH_4^+ + fNH_3$ (Fig. 2). In case 2, with complete nitrification, we find a more clear reduction in surface water pH, [Alk], and [DIC] relative to the control simulation (Figs. 2 and 3). The lower surface water [DIC] arises because the negative [Alk] perturbations raise $[pCO_2]$ and drive a perturbation efflux of CO_2 into the atmosphere, counter to the anthropogenic CO_2 flux. The negative Δ[DIC] perturbations are comparable, although slightly smaller than Δ[Alk] in an absolute sense, so that pH still declines but with significantly smaller amplitude than would occur from the original Δ[Alk] perturbation alone. The largest surface water anomalies are found in coastal regions surrounding the emission areas, with trends $\Delta pH/\Delta t$ of -0.02 to -0.12×10^{-3} pH units·y^{-1}, $\Delta[\text{Alk}]/\Delta t$ of -0.05 to -0.40 meq·m^{-3}·y^{-1}, and $\Delta[\text{DIC}]/\Delta t$ of -0.05 to -0.30 mmol·m^{-3}·y^{-1}. For comparison, the temporal trends in the anthropogenic CO_2 control simulation are $\Delta pH/\Delta t$ of -0.8 to -1.8×10^{-3} pH units·y^{-1} and $\Delta[\text{DIC}]/\Delta t$ of $+0.4$ mmol·m^{-3}·y^{-1} near the poles to $+1.2$ mmol·m^{-3}·y^{-1} in the subtropics.

Biological feedbacks depend on three factors: (*i*) the extent to which nitrification transforms excess NH_4^+ into NO_3^-; (*ii*) vertical redistribution of the excess nitrogen by means of biological nitrogen uptake in the surface, particle sinking, and subsurface remineralization; and (*iii*) biological drawdown of surface [DIC] from eutrophication. The effect of primary production on alkalinity depends on the source of nitrogen (31, 32). NO_3^--supported growth produces alkalinity (+1:1 eq/mol), and NH_4^+-supported growth removes alkalinity (−1:1 eq/mol):

$$106CO_2 + 16NO_3^- + 138H_2O \rightarrow \text{organics} + 16OH^- + 138O_2 \quad \textbf{[10]}$$

$$106CO_2 + 16NH_4^+ + 106H_2O \leftrightarrow \text{organics} + 16H^+ + 106O_2. \quad \textbf{[11]}$$

Alkalinity sources/sinks from phosphorus uptake and release are an order of magnitude smaller. Note that the alkalinity changes resulting from biological nitrogen uptake are opposite in sign to those generated directly by the original atmospheric deposition flux (Eq. **7**). Eventually, most of the extra organic nitrogen will be transported downward and remineralized in subsurface waters, releasing excess NH_4^+ that is almost immediately nitrified to NO_3^- in oxygenated waters.

The net effect of biological nitrogen cycling (case 3) is to reduce surface Δ[Alk] caused by atmospheric nitrogen deposition and to redistribute Δ[Alk] downward through the water column (Fig. 2). The impact, however, does not qualitatively alter the surface water alkalinity perturbations. The strongest negative surface Δ[Alk] anomalies in case 3 are somewhat smaller than those in case 2 but with greater spatial variability and some regions of positive trends (Fig. 3). Some of the spatial variability reflects the patterns of surface nutrient utilization, iron limitation, and the preferential biological uptake of NH_4^+ over NO_3^-. The increase in ocean nitrogen inventory in case 3 is smaller than the cumulative atmospheric nitrogen deposition of 2.7 Tmol·N·y^{-1} because elevated surface NO_3^- and productivity reduces simulated N_2 fixation by 0.6 Tmol·N·y^{-1} and increases denitrification by 0.1 Tmol·N·y^{-1}. Overall, nitrification modulates the acid/base signal from atmospheric nitrogen deposition, and $f\text{Alk}_{\text{nitrif}}$ with net alkaline effects everywhere is a reasonable approximation for the vertically integrated alkalinity sink in most locations.

Increased primary production stimulated by atmospheric nitrogen deposition lowers surface DIC with a ratio of ≈6.6 C/N (mol/mol) (Eqs. **10** and **11**). This results in qualitatively different solutions for pH and air–sea CO_2 flux perturbations (case 3; Fig. 3). The negative Δ[DIC] anomalies are amplified substantially relative to case 2 in some regions, with $\Delta[\text{DIC}]/\Delta t$ trends of -0.3 to -0.5 mmol·m^{-3}·y^{-1} over large areas. In many locations, Δ[DIC] decreases faster than Δ[Alk] and thus reverses the sign of the ΔpH signal, with $\Delta pH/\Delta t$ typically ranging from -0.2 to $+0.2 \times 10^{-3}$ pH units·y^{-1}. The case 3 spatial fields are also considerably more patchy, reflecting small-scale readjustments in model primary production, subsurface nutrients, and DIC.

Implications and Future Research

On a global scale, the alterations in surface water chemistry from anthropogenic nitrogen and sulfur deposition are only a few percent of the ocean acidification and Δ[DIC] increases expected from the oceanic uptake of anthropogenic CO_2. However, impacts on seawater chemistry can be much more substantial in coastal waters, on the order of 10–50% or more of the anthropogenic CO_2-driven changes near the major source regions and in marginal seas. Although there are certainly caveats with the simulated coastal signals because the global ocean model does not fully resolve complex coastal physical and biological dynamics, the coastal amplification is clear. Ocean acidification is thought to be a

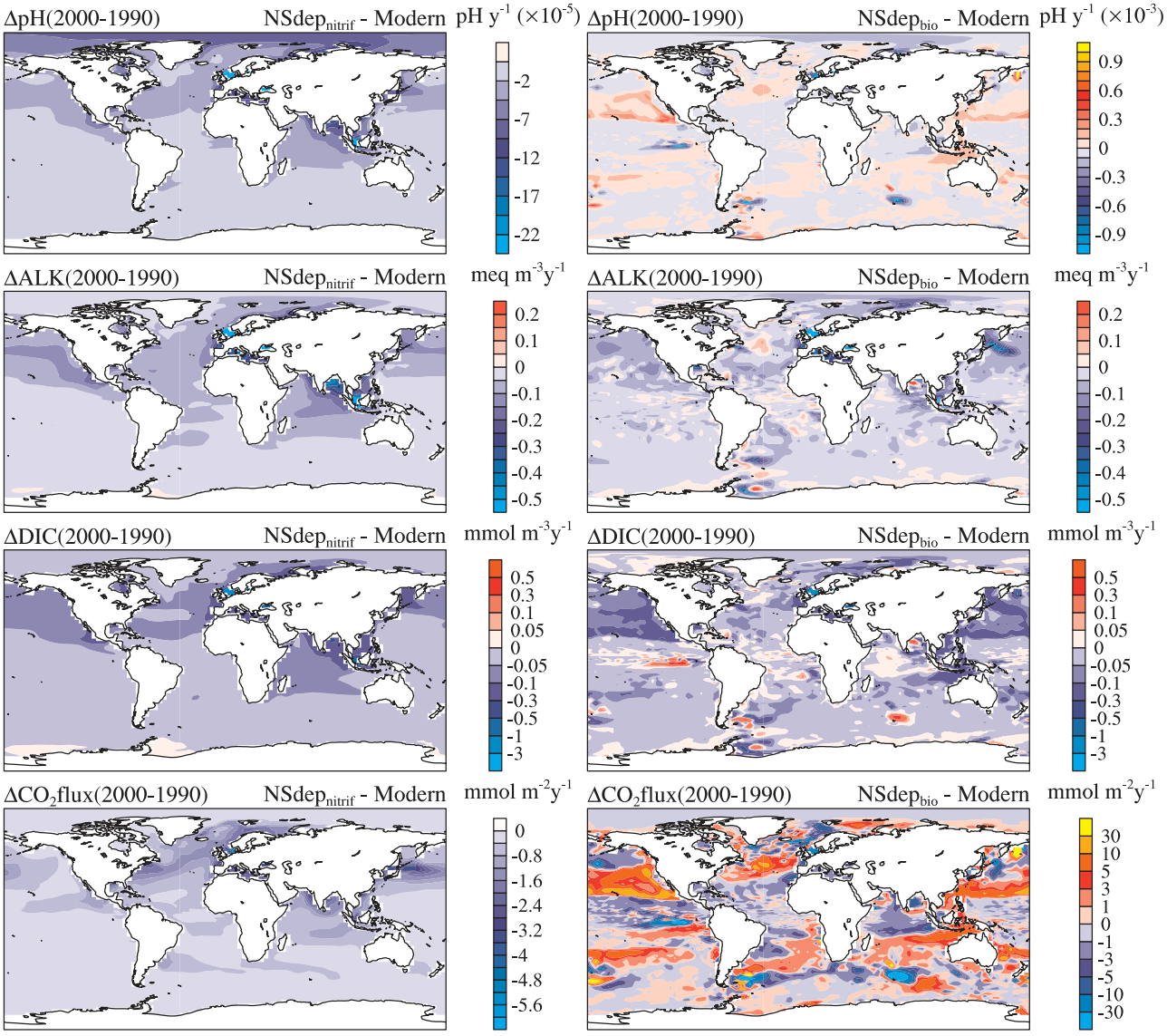

Fig. 3. Perturbation maps of simulated surface water pH, DIC, and total alkalinity trends and air–sea CO_2 flux due to anthropogenic atmospheric nitrogen and sulfur deposition.

significant threat to ecosystems, including coral reefs and coastal benthic and planktonic foodwebs dominated by calcifying organisms (10–13). Our study highlights the need to also consider the effects of non-CO_2 acidification sources from atmospheric nitrogen and sulfur deposition, both through their direct effects on reducing ocean alkalinity and their indirect effects through nitrogen fertilization of marine phytoplankton.

Uncertainties regarding the magnitude of non-CO_2 ocean acidification arise from errors in the anthropogenic sulfur and nitrogen deposition fluxes to the ocean, ocean circulation, and marine biogeochemical responses. Global deposition depends strongly on total emissions, with emission ranges of approximately ±16% for NO_x (total plus lightning) (7, 33), ±27% for NH_x (7, 34), and ±20% for SO_2 (35). Spatial differences in emissions and atmospheric transport pathways will change the downwind deposition fluxes to the oceans. The overall spatial patterns are generally similar across most models but can vary locally because of small shifts in steep deposition gradients. For example, sulfate residence times for models range between 3 and 5 days (35), with our model at 3.4 days. This means that deposition to remote regions in other models could be larger, but that uncertainties should be within ≈50%, even in remote regions. The response of seawater carbonate thermodynamics to acidification is well constrained. Better estimates of the uncertainties due to ocean circulation and biology require exploration of the effect in other numerical models and against field observations.

Here we highlight the first-order impacts associated with anthropogenic atmospheric nitrogen and sulfur. More comprehensive studies on global change and coastal acid/base chemistry would need to include a range of additional processes. The extent of atmospheric neutralization of acidic compounds may be varying because of changes in mineral dust emissions and alkaline fly ash from coal-fired power plants. There is evidence, for example, of reduced atmospheric deposition of basic cations (e.g., Ca^{2+}) (36). Although much of the acidity flux that falls on land will likely be neutralized by soils, some fraction may be transported to the ocean (10, 11, 29), and there are substantial riverine inputs of anthropogenic nitrogen and organic matter to the coastal domain (27, 30, 37). In the water column, second-order biological effects arise from altered rates of nitrogen fixation, water-column and sediment denitrification, calcification, and $CaCO_3$ remineralization (14, 15, 38–40).

Methods

Preindustrial and current nitrogen deposition (including nitrate and ammonia) are simulated (33) in the MOZART model (41), based on climate simulations from the Parallel Climate Model (42) for 1890 and 1990, respectively. Emissions for both preindustrial and present-day come from the EDGAR–HYDE inventory (43). Present-day emissions of ammonia follow ref. 7, whereas preindustrial emissions are assumed to be zero. For the sulfate species, simulations are conducted within the Community Atmospheric Model (CAM3) (44), using sulfate chemistry based on ref. 45. Emissions for preindustrial and current climate for sulfur are based on ref. 46, and the preindustrial and current climates were simulated by using slab ocean model versions (47).

The ocean model combines a state-of-the-art marine ecosystem module (48) with phytoplankton functional groups (pico/nanoplankton, diatoms, diazotrophs, and calcifiers), multiple limiting nutrients (N, P, Si, and Fe), zooplankton, and several detrital pools. The model explicitly tracks both NO_3^- and NH_4^+ pools and includes nitrification, nitrogen fixation, and water-column denitrification (39, 49). The biogeochemistry module (50) has full carbonate system thermodynamics (21), and air–sea CO_2 fluxes follow a quadratic wind-speed gas exchange relationship. The ecobiogeochemistry is embedded in the low-resolution (zonal 3.6°; meridional 0.8°–1.8°; 25 vertical layers with a 12-m-thick surface layer) National Center for Atmospheric Research ocean physical model (CCSM3.1), based on the Parallel Ocean Program (51). This model is integrated with a repeat annual cycle of surface forcing based on National Centers for Environmental Prediction reanalysis and satellite data products (52–54).

This work was supported by National Aeronautics and Space Administration Grant NNG05GG30G and National Science Foundation (NSF) Grant ATM06-28582 (to S.C.D. and I.L.), National Oceanic and Atmospheric Administration Grant GC05-285 (to R.A.F.), and NSF Grants EAR02-23509 and ATM04-39051 (to F.T.M.). The National Center for Atmospheric Research is supported by the NSF.

1. Intergovernmental Panel on Climate Change (2001) *Climate Change 2001: The Scientific Basis*, eds Houghton JT, Ding Y, Griggs DJ, Noguer M, van der Linden PJ, Dai X, Maskell K, Johnson CA (Cambridge Univ Press, New York).
2. Mackenzie FT (1995) in *Biotic Feedbacks in the Global Climatic System*, eds Woodwell G, Mackenzie FT (Oxford Univ Press, New York), pp 22–46.
3. Schlesinger WH (1997) *Biogeochemistry: An Analysis of Global Change* (Academic, San Diego).
4. National Acid Precipitation Assessment Program (1991) *Acidic Deposition: State of Science and Technology*, ed Irving PM (Govt Printing Office, Washington, DC), Vol 1.
5. Howarth RW, Billen G, Swaney D, Townsend A, Jaworski N, Lajtha K, Downing JA, Elmgren R, Caraco N, Jordan T, *et al.* (1996) *Biogeochemistry* 35:75–139.
6. Rodhe H, Dentener F, Schulz M (2002) *Environ Sci Technol* 36:4382–4388.
7. Dentener F, Drevet J, Lamarque JF, Bey I, Eickhout B, Fiore AM, Hauglustaine D, Horowitz LW, Krol M, Kulshrestha UC, *et al.* (2006) *Global Biogeochem Cycles* 20:GB4003.
8. Likens GE, Bormann HF, Johnson NM (1981) in *Some Perspectives of the Major Biogeochemical Cycles*, ed Likens GE (Wiley, New York), SCOPE Report No 17, pp 93–112.
9. Driscoll CT, Lawrence GB, Bulger AJ, Butler TJ, Cronan CS, Eagar C, Lambert KF, Likens GE, Stoddard JL, Weathers KC (2001) *Biosciences* 51:180–198.
10. Galloway JN (2001) *Water Air Soil Pollut* 130:17–24.
11. Galloway JN (2003) in *Interactions of the Major Biogeochemical Cycles*, eds Melillo JM, Field CB, Moldan B (Island Press, Washington, DC), pp 259–272.
12. Orr JC, Fabry VJ, Aumont O, Bopp L, Doney SC, Feely RA, Gnanadesikan A, Gruber N, Ishida A, Joos F, *et al.* (2005) *Nature* 437:681–686.
13. Kleypas JA, Feely RA, Fabry VJ, Langdon C, Sabine CL, Robbins LL (2006) *Impacts of Ocean Acidification on Coral Reefs and Other Marine Calcifiers: A Guide for Future Research* (Univ Corp Atmos Res, Boulder, CO).
14. Feely RA, Sabine CL, Lee K, Berelson W, Kleypas J, Fabry VJ, Millero FJ (2004) *Science* 305:362–366.
15. Andersson AJ, Mackenzie FT, Lerman A (2006) *Global Biogeochem Cycles* 20:GB1S92.
16. Jickells TD (1998) *Science* 281:217–222.
17. Zeebe RE, Wolf-Gladrow D (2005) *CO_2 in Seawater: Equilibrium, Kinetics, Isotopes* (Elsevier, Amsterdam).
18. Sabine CL, Feely RA, Gruber N, Key RM, Lee K, Bullister JL, Wanninkhof R, Wong CS, Wallace DWR, Tilbrook B, *et al.* (2004) *Science* 305:367–371.
19. Dickson AG (1981) *Deep-Sea Res* 28:609–623.
20. Morel FMM (1983) *Principles of Aquatic Chemistry* (Wiley, New York).
21. Department of Energy (1994) *Handbook of Methods for the Analysis of the Various Parameters of the Carbon Dioxide System in Sea Water*, eds Dickson AG, Goyet C (ORNL/CDIAC-74) (Oak Ridge National Laboratory, US Dept Energy, Oak Ridge, TN). Available at http://cdiac.ornl.gov/oceans/handbook.html.
22. Morse JW, Mackenzie FT (2006) *Geochemistry of Sedimentary Carbonates* (Elsevier, Amsterdam).
23. Nakicenovic N, Alcamo J, Davis G, de Vries B, Fenhann J, Gaffin S, Gregory K, Grübler A, Jung TY, Kram T, *et al.* (2000) *Emissions Scenarios: A Special Report of Working Group III of the Intergovernmental Panel on Climate Change* (Cambridge Univ Press, New York).
24. Doney SC (1999) *Global Biogeochem Cycles* 13:705–714.
25. Mikaloff Fletcher SE, Gruber N, Jacobson AR, Doney SC, Dutkiewicz S, Gerber S, Follows M, Joos F, Lindsay K, Menemenlis D, *et al.* (2006) *Global Biogeochem Cycles* 20:GB2002.
26. Ver LM, Mackenzie FT, Lerman A (1999) *Am J Sci* 299:762–801.
27. Mackenzie FT, Ver LM, Lerman A (2002) *Chem Geol* 190:13–32.
28. Paerl HW (1993) *Can J Fish Aquat Sci* 50:2254–2269.
29. Mackenzie FT, Ver LM, Sabine C, Lane M, Lerman A (1993) in *Interactions of C, N, P, and S Biogeochemical Cycles and Global Change*, eds Wollast R, Mackenzie FT, Chou L (Springer, Berlin), pp 1–62.
30. Galloway JN, Dentener FJ, Capone DG, Boyer EW, Howarth RW, Seitzinger SP, Asner GP, Cleveland CC, Green PA, Holland EA, *et al.* (2004) *Biogeochemistry* 70:153–226.
31. Brewer PG, Goldman JC (1976) *Limnol Oceanogr* 21:108–117.
32. Goldman JC, Brewer PG (1980) *Limnol Oceanogr* 25:352–357.
33. Lamarque J-F, Kiehl JT, Brasseur GP, Butler T, Cameron-Smith P, Collins WD, Collins WJ, Granier C, Hauglustaine D, Hess PG, *et al.* (2005) *J Geophys Res* 110:D19303.
34. Bouwman AF, Lee DS, Asman WAH, Dentener FJ, Van Der Hoek KW, Olivier JGJ (1997) *Global Biogeochem Cycles* 11:561–588.
35. Textor C, Schulz M, Guibert S, Kinne S, Balkanski Y, Bauer S, Berntsen T, Berglen T, Boucher O, Chin M, *et al.* (2006) *Atmos Chem Phys* 6:1777–1813.
36. Hedin LO, Granat L, Likens GE, Adri Buishand T, Galloway JN, Butler TJ, Rodhe H (1994) *Nature* 367:351–354.
37. Boyer EW, Howarth RW, Galloway JN, Dentener FJ, Green PA, Vorosmarty CJ (2006) *Global Biogeochem Cycles* 20:GB1S91.
38. Fennel K, Wilkin J, Levin J, Moisan J, O'Reilly J, Haidvogel D (2006) *Global Biogeochem Cycles* 20:GB3007.
39. Moore JK, Doney SC (2007) *Global Biogeochem Cycles* 21:GB2001.
40. Krishnamurthy A, Moore JK, Luo C, Zender CS (2007) *J Geophys Res* 112:G02019.
41. Horowitz LW, Walters S, Mauzerall DL, Emmons LK, Rasch PJ, Granier C, Tie X, Lamarque J-F, Schultz MG, Tyndall GS, *et al.* (2003) *J Geophys Res* 108:4784.
42. Washington WM, Weatherly JW, Meehl GA, Semtner AJ, Jr, Bettge TW, Craig AP, Strand WG, Jr, Arblaster J, Wayland VB, James R, Zhang Y (2000) *Clim Dyn* 16:755–774.
43. van Aardenne JA, Dentener FJ, Olivier JGJ, Klein CGM (2001) *Global Biogeochem Cycles* 15:909–928.
44. Collins WD, Blackmon M, Bitz CM, Bonan GB, Bretherton CS, Carton JA, Chang P, Doney S, Hack JJ, Kiehl JT, *et al.* (2006) *J Clim* 19:2122–2143.
45. Rasch PJ, Collins W, Eaton BE (2001) *J Geophys Res* 106:7337–7355.
46. Smith SJ, Conception E, Andres R, Lurz J (2004) *Historical Sulfur Dioxide Emissions 1850–2000: Methods and Results* (Pacific Northwest Natl Lab, Richland, WA), PNNL-14537.
47. Kiehl J, Shields C, Hack J, Collins W (2006) *J Clim* 19:2584–2596.
48. Moore JK, Doney SC, Lindsay K (2004) *Global Biogeochem Cycles* 18:GB4028.
49. Moore JK, Doney SC, Lindsay K, Mahowald N, Michaels AF (2006) *Tellus B Chem Phys Meteorol* 58:560–572.
50. Doney SC, Lindsay K, Fung I, John J (2006) *J Clim* 19:3033–3054.
51. Smith R, Gent P (2004) *Reference Manual for the Parallel Ocean Program (POP)* (Los Alamos Natl Lab, Los Alamos, NM), LAUR-02-2484.
52. Doney SC, Large WG, Bryan FO (1998) *J Clim* 11:1420–1441.
53. Large WG, Yeager SG (2004) *Diurnal to Decadal Global Forcing for Ocean and Sea-Ice Models: The Data Sets and Flux Climatologies* (Natl Center Atmos Res, Boulder, CO), Technical Note NCAR/TN-460+STR.
54. Doney SC, Yeager S, Danabasoglu G, Large WG, McWilliams JC, *J Phys Oceanogr* 37:1918–1938.